PAN
POLSKA AKADEMIA NAUK
JOURNAL OF WATER AND LAND DEVELOPMENT
e-ISSN 2083-4535
ITP-PIB
Polish Academy of Sciences (PAN) Institute of Technology and Life Sciences – National Research Institute (ITP – PIB)

JOURNAL OF WATER AND LAND DEVELOPMENT
DOI: 10.24425/jwld.2021.138185
2021, No. 50 (VI–IX): 85–97

Performance evaluation of HEC-HMS model for continuous runoff simulation of Gilgel Gibe watershed, Southwest Ethiopia

Sewmehon Sisay Fanta ✉, Tolera Abdissa Feyissa

Jimma University, Faculty of Civil and Environmental Engineering, Institute of Technology, Jimma, Ethiopia

RECEIVED 11.11.2020 REVIEWED 10.03.2021 ACCEPTED 09.07.2021

Abstract: Hydrological models are widely used for runoff simulation throughout the world. The objective of this study is to check the performance of the HEC-HMS model for continuous runoff simulation of Gilgel Gibe watershed. It includes sensitivity analysis, calibration, and validation. The model calibration was conducted with data from the year 1991 to 2002 and validated for the year 2003 to 2013 period using daily observed stream flow near the outlet of the watershed. To check the consistency of the model, both the calibration and validation periods were divided into two phases. The sensitivity analysis of parameters showed that curve number (CN) and wave travel time (*K*) were the most sensitive, whereas channel storage coefficient (*x*) and lag time (*t*lag) were moderately sensitive. The model performance measured using Nash–Sutcliff Efficiency (*NSE*), Percentage of Bias (*PBIAS*), correlation coefficient (R^2), root mean square error (*RMSE*), and Percentage Error in Peak (*PEP*). The respective values were 0.795, 8.225%, 0.916, 27.105 $m^3 \cdot s^{-1}$ and 7.789% during calibration, and 0.795, 23.015%, 0.916, 29.548 $m^3 \cdot s^{-1}$ and –19.698% during validation. The result indicates that the HEC-HMS model well estimated the daily runoff and peak discharge of Gilgel Gibe watershed. Hence, the model is recommended for continuous runoff simulation of Gilgel Gibe watershed. The study will be helpful for efficient water resources and watershed management for Gilgel Gibe watershed. It can also be used as a reference or an input for any future hydrological investigations in the nearby un-gauged or poorly gauged watershed.

Keywords: calibration, Gilgel Gibe, HEC-HMS, runoff simulation, sensitivity analysis, validation

INTRODUCTION

Rainfall-runoff process is affected by every physical characteristic of the watershed including watershed area, surface slope, land use/ land cover, vegetation, geology, soil type, and hydro-metrological variables [McColl, Aggett 2006]. Due to insufficiency or poor quality and reliability of hydrological data and watershed parameters, it becomes a major challenge to predict runoff response to rainfall events [Majidi 2012]. The better alternative solution to this challenge is the use of hydrological models [Yener *et al.* 2007].

There are different types of hydrological models based on different criteria. According to the mathematics involved, hydrological models are divided into two broad categories, viz: deterministic and stochastic [Kumarasamy, Belmont 2018].

The deterministic models generate only a single outcome from the simulation of one set of input parameter values [Meresa 2019]. Stochastic models allow some randomness on the outcome because of the uncertainty in input variables, boundary conditions, or model parameters.

Based on the processes description, the deterministic model are classified into three major classes [Derdous *et al.* 2018]. The first one is the lumped model which evaluates the basin response at outlet of the watershed [Ibrahim-Bathis, Ahmed 2016]. The second is the distributed model which predicts the basin response by discretizing the basin into many elements. It gives detail and potentially more correct descriptions of the hydrological processes. [Meresa 2019]. The last one is the semi-distributed model. In this model, parameters are allowed to vary partially in the watershed. HEC-HMS, SWAT, and SWMM are good examples of semi-distributed models [Tassew *et al.* 2019].

HEC-HMS is a numerical and semi-distributed hydrologic model developed by the United States Army Corps of Engineers [USACE 2010]. It is applied in several watershed of the world for event based and continuous runoff simulation [Gyawali *et al.* 2013; Rahman *et al.* 2017]. Several studies conducted in different regions of the world under different watershed characteristics showed the successfulness of HEC-HMS model in runoff simulation [Halwatura, Najim 2013; Majidi 2012; Sintayehu 2015; Tassew *et al.* 2019; Zelelew, Melese 2018].

Although several studies were conducted in different river basins across the world, only a very little attention is given for modelling Ethiopian river basins using HEC-HMS [Tassew *et al.* 2019]. According to Teklu *et al.* [2016], the Gilgel Gibe watershed runoff is highly varying temporally and spatially due to natural and manmade involvements such as agricultural activity, climate change and urbanization. Although watershed development programs and water resource projects are ongoing at present, the output depends upon accurate spatial and temporal distributed runoff information.

Zelelew and Melese [2018] and Laouacheria and Mansouri [2015] showed that the response of HEC-HMS model varies in different regions of the world, which depends upon the spatial and temporal variation of climate and watershed characteristics. This is due to the variation of the response of the methods involved for modelling losses, direct runoff, routing and base flow in different regions of the world [Verma *et al.* 2010]. Therefore, the objective of this study is to shows the suitability of HEC-HMS model for continuous runoff simulation of Gilgel Gibe watershed.

When it is planned to use a certain hydrological model, its suitability for the watershed area of interest is the basic criteria to be considered. Hence, checking the HEC-HMS model performance is crucial for efficient water resources and watershed management. It also helps to develop different watershed and water resources management scenario. The methodologies and results of this study can also be used as an input for runoff estimation, flood forecasting, water balance and watershed management in un-gauged or poorly gauged watershed having similar hydro metrological and morphologic characteristics with Gilgel Gibe watershed.

MATERIALS AND METHODS

DESCRIPTION OF THE STUDY AREA

Gilgel Gibe watershed is located in southwestern highland of Ethiopia. Geographically, the watershed lies between 7°19'07.15" and 8°12'09.49" N latitudes and 36°31'42.60" and 37°25'16.05" E longitudes. It has a total area of 4218 km^2 and an average elevation of 1700 m a.m.s.l.

The drainage density of the watershed varies from 0 to 1.16 m^{-1} from the boundaries towards the center of the watershed due to high permeability of the soil. Figure 1 shows the geographic location of Gilgel Gibe watershed.

The climatic condition varies from sub-humid warm to hot. The collected data analysis indicates that the minimum-recorded monthly average rainfall was 35 mm in January, but the maximum monthly average recorded precipitation was 222 mm in July. Figure 2 shows the monthly average rainfall distribution of Gilgel Gibe watershed from the year 1991 to 2017.

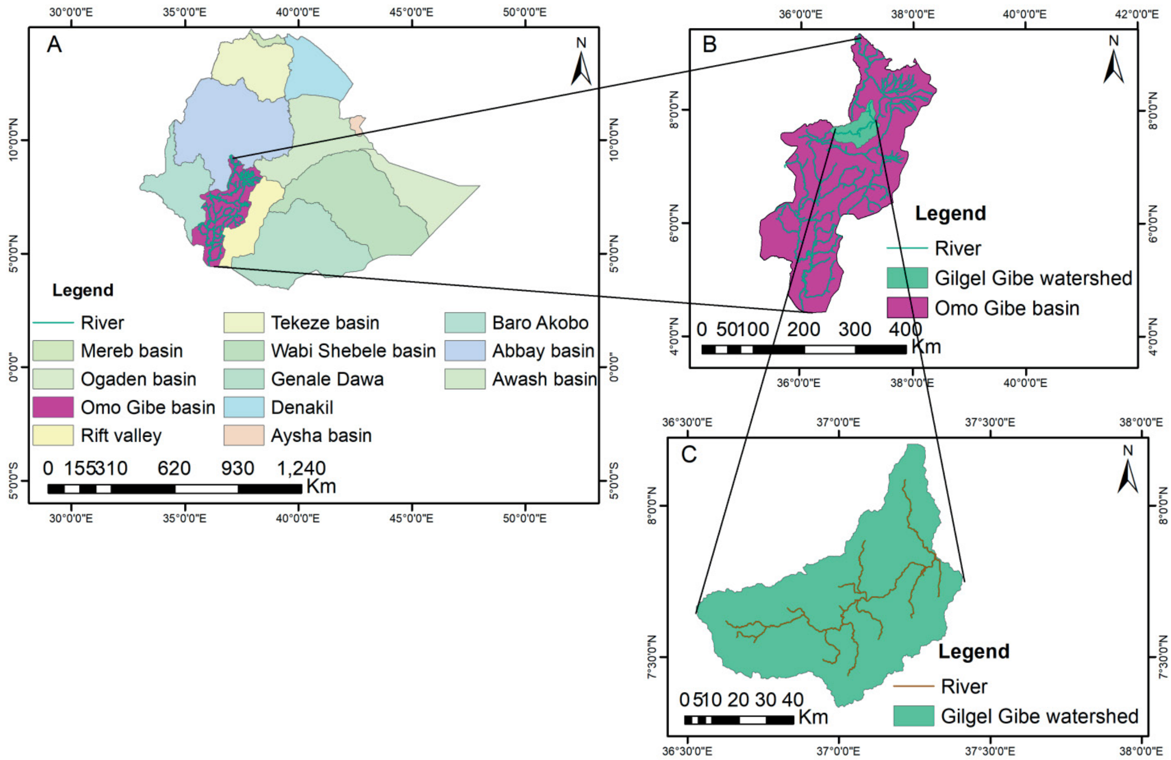

Fig. 1. Location map of Gilgel Gibe watershed: A) Ethiopian river basin, B) Omo Gibe basin, and C) Gilgel Gibe watershed; source: own elaboration

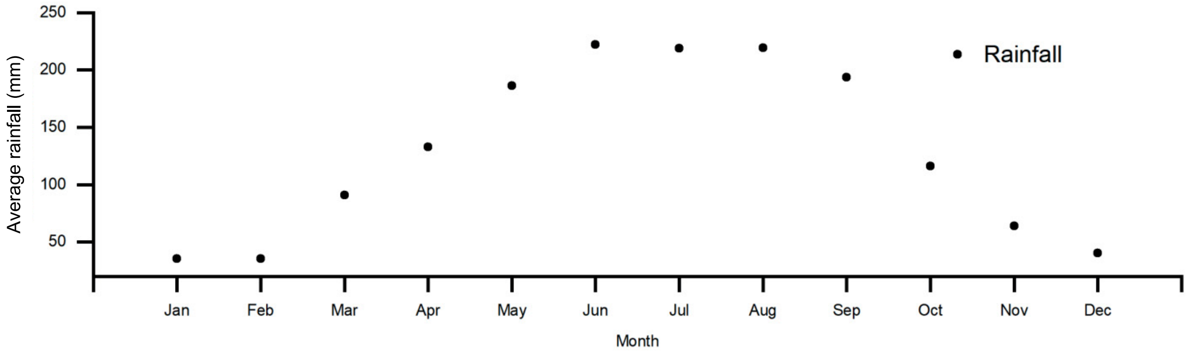

Fig. 2. Monthly average rainfall of Gilgel Gibe watershed (1991–2017); source: own elaboration

DATA COLLECTION AND ANALYSIS

Higher-resolution Digital Elevation Model (DEM) is ideal to study the hydrological response of watersheds. Therefore, 12.5 m × 12.5 m resolution DEM covering the study area was obtained from Alaska satellite facility service.

The surface slope grid was generated from the DEM. To get insight on the variation of watershed responses owing to slope difference between the watersheds, slope of the watershed was reclassified into gentle (0–9°), steep (9–20°), and excessive (>20°). The classification was based on slope classes defined by Scott and Hofer [1995].

The analysis indicates that 52.3% of the watershed has gentle slope, 37.3% steep slope, and 10.5% excessive slope. Figure 3 shows the DEM in which elevation is measured in meter and slope grid map of Gilgel Gibe watershed which was measured in degree.

Data on Land Use/Land Cover (LU/LC) and respective soil for the study area were taken from the office of Ethiopian Mapping Agency and GIS department of Ministry of Water, Irrigation, and Electricity of Ethiopia, respectively.

Soil data analysis indicates that, the watershed has seven major soil types. Fig. 4a shows the soil types of Gilgel Gibe watershed. Eutric fluvisols are the dominant soil type which covers 34% of the study area where as Eutric cambisols cover only 0.65% of the watershed.

Major categories of LU/LC of the study area are agricultural, forestry, grassland, urban areas, and water bodies. Agriculture is the dominant land use type, which covers 90% of the watershed. Figure 4b shows the major LU/LC types of the watershed.

The HEC-HMS model requires meteorological and hydrological data at hourly or daily time step to simulate runoff. For this study, daily meteorological data covering 27 years for seven stations (Asendabo, Dedo, Jimma, Omo Nada, Limu Genet, Shebe, and Sekoru) were collected from the National Meteorology Agency of Ethiopia. Among other stations, which are available in and around the watershed, these stations were selected based on the number of missing data where stations having 85% of full data record are selected for this study. The location, elevation, duration, and the percentage of missing data for each station are summarized in Table 1.

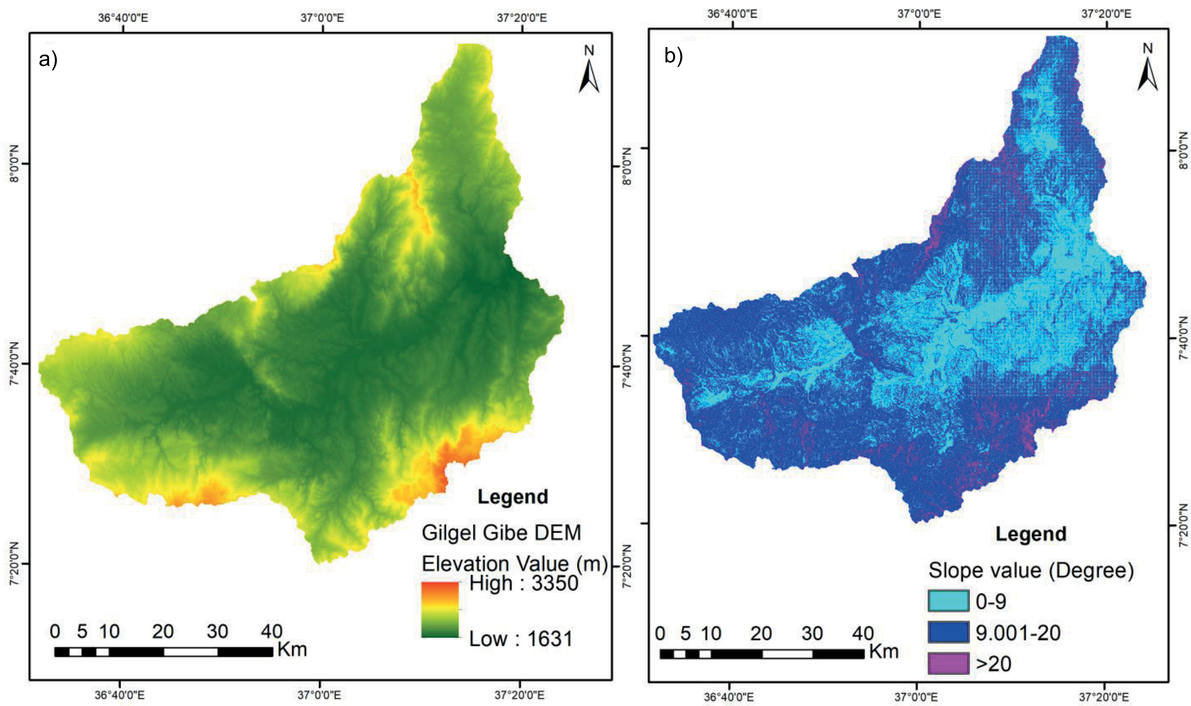

Fig. 3. DEM and slope grid map of Gilgel Gibe watershed: A) DEM, and B) watershed slope; source: own study

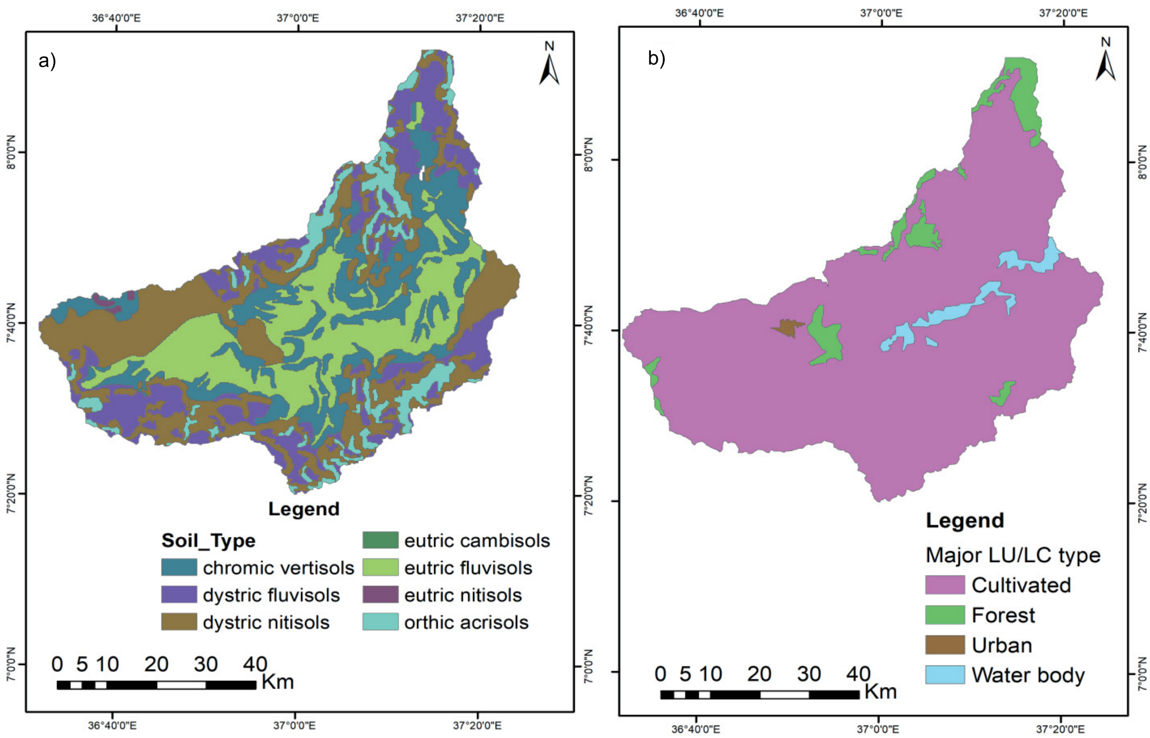

Fig. 4. Soil and Land Use/Land Cover (LU/LC) map of Gilgel Gibe watershed: a) soil map, b) LU/LC map; source: own study

Table 1. Summarized information of the selected meteorological stations

Station No.	Station name	Latitude (°)	Longitude (°)	Elevation (m)	Duration (year)	Missing data (%)
1	Sekoru	7.92	37.42	1928	1991–2017	12.5
2	Limu Genet	8.07	36.95	1766	1991–2017	7.8
3	Asendabo	7.75	37.22	1764	1991–2017	5.5
4	Jimma	7.70	36.82	1718	1991–2017	4.4
5	Dedo	7.52	36.87	2210	1991–2017	8.5
6	Omo Nada	7.62	37.25	1838	1991–2017	10.65
7	Shebe	7.50	36.52	1813	1991–2017	13.5

Source: own study.

The daily stream flow for the period from the year 1991 to 2013 was collected from the hydrology department of Ministry of Water, Irrigation and Electricity of Ethiopia. The stream flow and rainfall data distribution shows missing values ranging from 4.4% to 13.5%, which are filled using different data filling techniques based on the nature of data distribution. Subsequently, the homogeneity test was conducted using Rainbow software to detect the variability of the data, which measures the cumulative deviation from the mean of the time series [Raes *et al.* 2006]. The result indicated the homogeneity of hydro-metrological data.

BASIN MODEL PREPARATION AND SPATIAL WATERSHED PARAMETER COMPUTATION

The basin model was prepared by terrain preprocessing and hydrologic processing functions of the HEC-GeoHMS terrain preprocessing was performed to delineate the watershed using the existing DEM. Hydrologic processing was also performed to extract CN and lag time.

COMPUTATION OF SUB-WATERSHED CURVE NUMBER

Runoff curve number is the main watershed parameter for the estimation of runoff. The curve number was generated by combining soil and land cover of the watershed. The final curve number grid map is shown in Figure 5. The CN value varies from 30 for urban area to 98 for water body. Figure 5 indicates the range of curve number in different colours.

The minimum curve number represented by flame red colour, which is for urban area, and the maximum curve number is represented by ultra-blue colour, which represents the curve number for water body. Subsequently, the weighted average value of CN for each sub-watershed computed using the parameter estimation tool of the HEC-GeoHMS.

COMPUTATION OF LAG TIME

The lag time (*t*lag) is one of the input parameters for the SCS unit hydrograph of the transform method. For this study, HEC--GeoHMS tool was used to compute the lag time for each

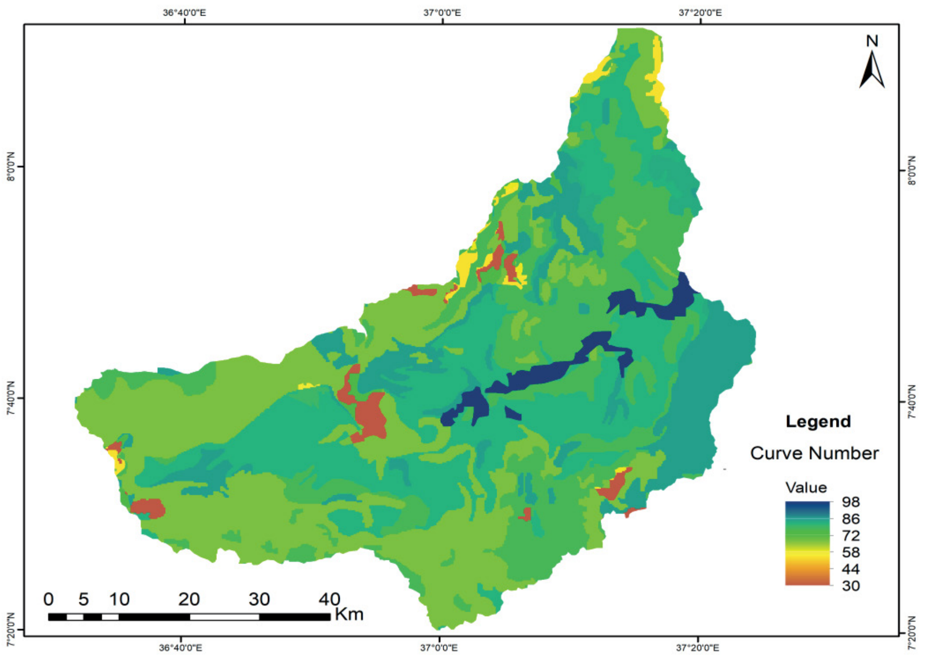

Fig. 5. Curve number grid map of Giglel Gibe watershed; source: own study

sub-watershed using the CN lag method. It relates lag time with other watershed parameters by equation (1) [MISHRA, SINGH 2013].

$$t\text{lag} = \frac{L^{0.8}(s+1)^{0.7}}{1900y^{0.5}} \tag{1}$$

where: *t*lag is the lag time (hour), *L* is the length from the outlet to divide along the longest drainage path (ft), *y* is the slope (%), and *s* is the saturated moisture content (inch).

The generated weighted *CN* value and lag time for each sub-watershed is shown in Table 2.

COMPUTATION OF WAVE TRAVEL TIME AND CHANNEL STORAGE COEFFICIENT

SONG *et al.* [2011] developed the following formula to determine the wave travel time (*k*) and channel storage coefficient (*x*) for parabolic channel section.

Table 2. Gilgel Gibe sub-watershed curve number and lag time

Sub-watershed	Curve number	Lag time (h)
SW1	81	3.55
SW2	84	3.32
SW3	86	3.03
SW4	86	3.73
SW5	84	3.67
SW6	85	2.31
SW7	83	3.10
SW8	86	3.93
SW9	85	3.08
SW10	91	2.92
SW11	86	3.04

Source: own study.

$$k = \frac{0.69n^{0.6}Lc^{0.4}}{3600Qo^{0.2}s^{0.3}} \tag{2}$$

$$x = \frac{1}{2} - \frac{0.35{Q_o}^{0.3}n^{0.6}}{s^{1.3}c^{0.8}L} \tag{3}$$

where: *n* is the Manning roughness coefficient; *L* is the length of channel; *c* is a coefficient whose value ranges from 4.71 to 4.8 and Q_o is the reference discharge given by:

$$Q_o = Q_b + 0.5(Q_p - Q_b) \tag{4}$$

where: Q_b and Q_p are the respective minimum and maximum discharge carried by the channel.

These values are used as initial parameters during the initial simulation. Estimation of allow partial parameter variation in the watershed.

HEC-HMS MODEL COMPONENTS

The major HEC-HMS Model components are basin model, meteorological model, control specifications, and input data (time series, paired data, and gridded data).

The basin model represents the hydrologic elements with their connectivity that characterizes the movement of water through the river. Since HEC-HMS is a semi-distributed model, Gilgel Gibe watershed was divided into eleven-sub watershed to allow partial parameter variation in the watershed. Figure 6 shows the basin model which was prepared using HEC-Geo HMS.

The basin model also consists of four major types of analytical components for the major hydrological processes. These are loss model, transform model, base flow model and routing model. For smaller streams and the mountainous watershed, the contribution of base flow to the stream is insignificant [Tassew *et al.* 2019]. Hence, it was not considered for this study.

SELECTION OF LOSS MODEL

In the HEC-HMS model, loss models for each sub-basin compute the amount of infiltration. There are four major types of loss models in HEC-HMS. For this study, the Soil Conservation Service-Curve Number (SCS-CN) loss model was selected due to the following reasons: (1) the major factors that affect runoff generation such as soil type, land use and treatment, surface condition and antecedent moisture condition are incorporated in a single CN value; (2) it provides a better result than the initial and constant loss model, which also requires fewer watershed parameters [Yener *et al.* 2007]. It is the most effective and convenient method of loss estimation [Khaniya *et al.* 2017].

The maximum retention and the basin characteristics are related through CN by equation (5) [Du *et al.* 2012; Mishra, Singh 2013; Verma *et al.* 2010].

$$Q = \frac{(P - 0.2S)^2}{(P + 0.8S)} \tag{5}$$

where P is the precipitation (mm) and S is the soil maximum retention potential (mm).

The soil maximum retention potential is a function of sub-watershed CN related by:

$$S = \frac{25400}{\text{CN}} - 254 \tag{6}$$

where CN is the basin curve number

SELECTION OF TRANSFORM MODEL

In the HEC-HMS model, the excess precipitation is transformed into runoff by the transform model. There are seven types of transform models. For this study, the Soil Conservation Service Unit Hydrograph (SCS-UH) model was selected for modelling direct runoff.

According to Ramly and Tahir [2015], this method is characterized by fewer parameter requirements. The appropriateness of the assumptions inherent in the model and its previous application in various watersheds around the globe were the other major criteria considered for the selection of this model. DU et al. [2012] stated that in SCS-UH runoff transformation model, the peak discharge of unit hydrograph peak (Up) is given by:

$$Up = C\frac{A}{Ttp} \tag{7}$$

where: A is the sub-watershed area, tp is time of peak, C is conversion constant.

The time of peak is a function of duration unit of excess precipitation given by:

$$tp = \frac{\Delta t}{2} + t\text{lag} \tag{8}$$

where: Δt is the simulation time step in HEC-HMS model.

Hence, Equation (8) indicates that lag time is the only required parameter for this model.

SELECTION OF ROUTING MODEL

Channel routing model predicts the downstream hydrograph using the upstream hydrograph as a boundary condition [Pechlivanidis *et al.* 2011].

Among the routing models available in HEC-HMS, the Muskingum routing model was selected for this study. It is preferred over other routing methods when there is a lack of physically observed site-specific parameters of the river [Roy *et al.* 2013]. It is also the most commonly used hydrologic routing model for natural channel [Skhakhfa, Ouerdachi 2016].

The model uses a simple finite difference approximation of the storage continuity equation, which can be expressed as:

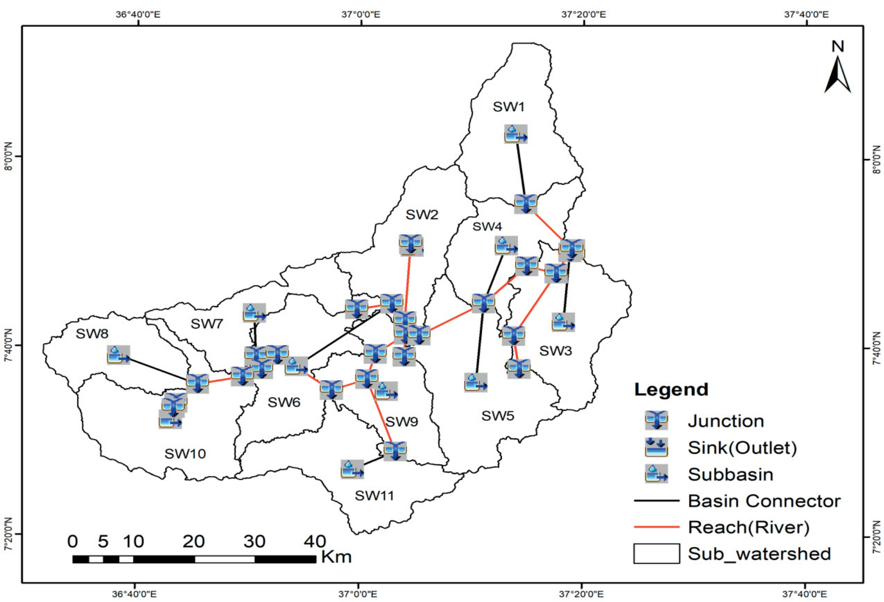

Fig. 6. Basin model of Gilgel Gibe watershed; source: own study

$$St = KOt + Kx(It - Ot) = K[It + (1 - x)Ot] \quad (9)$$

where: K is the travel time of the flood wave (h), St is the storage in the channel at time t ($m^3 \cdot s^{-1}$), It is the inflow to the channel at time t ($m^3 \cdot s^{-1}$), Ot is the outflow from the channel at time ($m^3 \cdot s^{-1}$), and x is the channel storage coefficient.

METEOROLOGICAL AND TIME-SERIES DATA ENTRY METHODS

The distribution of precipitation over the whole watershed was specified using the gauge weight method. Thiessen polygon was constructed using Arc GIS 10.1. Figure 7 shows the sub-watershed Thiessen polygon for each precipitation contributing station.

The gauge weight of each rainfall contributing gauges is the ratio of the area of the polygon and the total area of each sub-watershed. The daily areal precipitation data were obtained by multiplying the gauge weight by gauge precipitation for each sub watershed. Table 3 also shows the rainfall contributing gauges in terms of gauge weight.

HEC-HMS MODE PERFORMANCE EVALUATION

Model performance evaluation includes sensitivity analysis, calibration, and validation [WALEGA 2013]. Sensitivity analysis was conducted to determine the most sensitive parameters for runoff generation. For this study, the sensitivity of CN, *t*lag, Muskingum (k) and Muskingum (x) were selected for sensitivity analysis based on the selected loss, transform and routing models respectively.

The computed initial values of the parameters were manually entered into the respective analytical components of HEC-HMS model. The simulation was conducted thereafter by

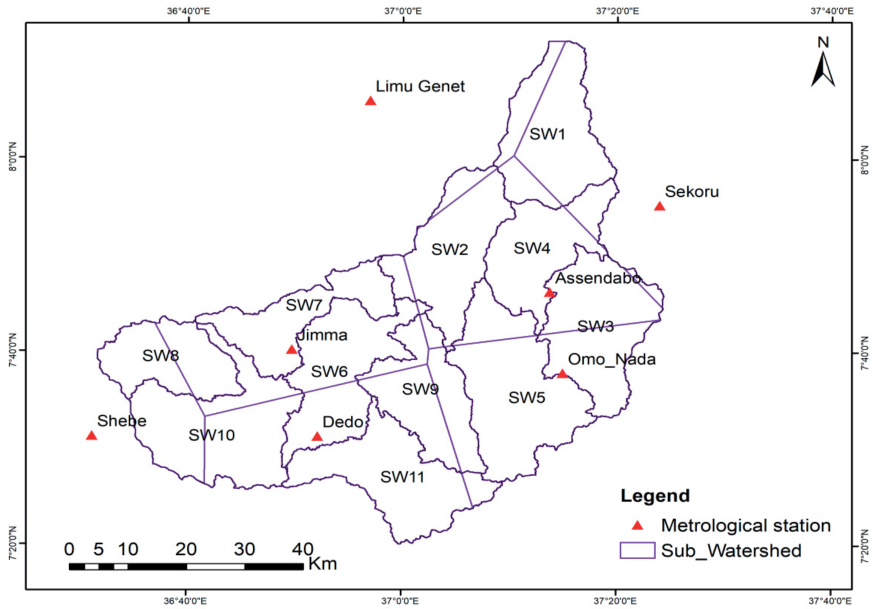

Fig. 7. Sub-watershed Thiessen polygons for precipitation contributing stations; source: own study

Table 3. Contributing stations and their assigned gauge weight for individual sub watershed

Sub-watershed	Contributing stations and their gauge weight						
	Asendabo	Dedo	Jimma	Limu Genet	Omo Nada	Sekoru	Shebe
SW1	0.13	0.00	0.00	0.20	0.00	0.68	0.00
SW2	0.82	0.00	0.08	0.09	0.01	0.00	0.00
SW3	0.51	0.00	0.00	0.00	0.46	0.03	0.00
SW4	0.84	0.00	0.00	0.00	0.00	0.16	0.00
SW5	0.18	0.00	0.00	0.00	0.82	0.00	0.00
SW6	0.01	0.38	0.61	0.00	0.00	0.00	0.00
SW7	0.00	0.00	1.00	0.00	0.00	0.00	0.00
SW8	0.00	0.00	0.48	0.00	0.00	0.00	0.52
SW9	0.04	0.47	0.16	0.00	0.33	0.00	0.00
SW10	0.00	0.44	0.20	0.00	0.00	0.00	0.36
SW11	0.00	0.94	0.00	0.00	0.06	0.00	0.00

Source: own study.

varying each parameter so that the most influential parameters could be separated.

The HEC-HMS model Version 4.2 has an optimization manager that allows automated model calibration. In this study, both manual and automatic calibrations were used to adjust each parameter value.

HEC-HMS MODEL PERFORMANCE EVALUATION CRITERIA

Different statistical tests of error functions have different objectives. Therefore, it is preferred to check the model performance using more than one and widely accepted error functions.

In this study, Nash and Sutcliffe efficiency (*NSE*), Root Mean Square Error (*RMSE*), Percent Bias (*PBIAS*), coefficient of determination (R^2), and Percent Error in Peak (*PEP*) were selected for model performance evaluation. It is important to use multiple evaluation criteria to minimize bias during model evaluation [KUMARASAMY, BELMONT 2018] several previous studies proved the widely applicability of this statistics for evaluation of different hydrological model [VERMA *et al.* 2010]. According to KUMARASAMY, BELMONT [2018], *NSE*, R^2 and *PBIAS* are effective model performance lumped metrics.

NSE is a measure of efficiency that relates the goodness-of-fit of the model to the variance of measured data. *NSE* can range from – ∞ to one and an efficiency of one indicates perfect equivalent between the observed and simulated discharge [ZOU *et al.* 2003]. Mathematically, it is expressed as:

$$NSE = 1 - \frac{\sum_{i=1}^{n} \left[Qoi - Qsi\right]^2}{\sum_{i=1}^{n} \left[Qoi - \overline{Qo}\right]^2} \quad (10)$$

where: *Qo* is the observed flow, *Qs* is the simulated flow $\overline{Qo}$ is the average of the observed flow, *i* is the time step, and *n* is the total number of time steps. Both observe and simulated flows measured in $m^3 \cdot s^{-1}$.

The R^2 value indicates the degree of correlation between the simulated and observed runoff [KUMARASAMY, BELMONT 2018]. Its value varies from zero to one, with higher values indicating a high degree of correlation. It has been widely used for model evaluation [ZHANG *et al.* 2013]. Mathematically, it is expressed as:

$$R^2 = \frac{\left[\sum_{i=1}^{n} \left(Qsi - \bar{Q}s\right)\left(Qoi - Qo\right)\right]^2}{\left[\sum_{i=1}^{n} \left(Qsi - \overline{Qs}\right)\right]^2 \left[\sum_{i=1}^{n} \left(Qoi - \overline{Qo}\right)\right]^2} \quad (11)$$

The *RMSE* is a commonly used measure of differences (residuals) between simulated and observed runoff values [MORIASI *et al.* 2007; ZHANG *et al.* 2013]. Mathematically, *RMSE* is expressed as:

$$RMSE = \sqrt{\frac{\sum_{i=1}^{n} \left(Qo - Qsi\right)^2}{n}} \quad (12)$$

The *PBIAS* measures the average tendency differences between the observed and simulated flow [MORIASI *et al.* 2007]. Mathematically, it is expressed as:

$$PBIAS = \sum_{i=1}^{n} \frac{(Qoi - Qsi)100}{\sum_{i=1}^{n} Qoi} \quad (13)$$

The *PEP* measures model performance by comparing the observed and simulated peak runoff value [USACE 2010].

$$PEP = \left|\frac{Qo(\text{peak}) - Qs(\text{peak})}{Qo(\text{peak})}\right| 100 \quad (14)$$

RESULTS AND DISCUSSION

SENSITIVITY ANALYSIS

Sensitivity analysis was conducted by varying respective parameters in each simulation trial. The model parameters were varied in the range of ±25% at 5% interval in each optimization trial.

The analysis indicates that CN and Muskingum *k* were the most sensitive parameters. A minor change in the values of this parameter altered the shape of simulated runoff hydrographs. This shows the dependency of runoff on land use/land cover, soil type, topography of the watershed and the channel characteristics. Channel storage coefficient and lag time are moderately sensitive parameters.

Figure 8 shows the response of percentage change of parameters value on runoff value. The result also shows that as the percentage change in CN and lag time values increases, the percentage change in runoff volume increases. Whereas, the increase in the value of Muskingum *k* and Muskingum *x* has inverse relation with the variation of runoff volume.

MODEL CALIBRATION

A long period of observed flow is preferred for model calibration and validation to check the consistency of the model performance in continuous runoff simulation.

The Predictive ability of HEC-HMS model is dependent on the spatial and temporal variation of morphological and hydrological characteristics of the watershed. Therefore, both the calibration and validation periods were divided into two phases to check the temporal variation of the optimum value of sensitive parameters. Moreover, the splitting of the calibration and validation period is important to check the consistency of the trend of the relationship between simulated and observed flow.

Because of that, the observed data from 1 January 1991 to 31 December 1996 and from 1 January 1997 to 31 December 2002 was used for the first and second phases of model calibration periods, respectively.

Initially, the model was allowed to run using the initial values of sensitive parameters. The difference between the observed and simulated runoff hydrograph was evaluated using *NSE*, R^2, *RMSE*, *PBIAS* and *PEP*. Their initial values were 0.05, 0.43, 93.73 $m^3 \cdot s^{-1}$ 65.45%, and 58.9% respectively. Since these values are below the acceptable level of accuracy, parameter adjustment conducted from initial sensitive parameters value using manual and optimization trial. The trial terminated at minimum difference in observed and simulated runoff hydrograph. The average values of optimum parameters for each phase are given in Table 4.

The average optimum value of the curve number scale factor is multiplied by the original curve number value to get the optimum curve number value for each sub watershed.

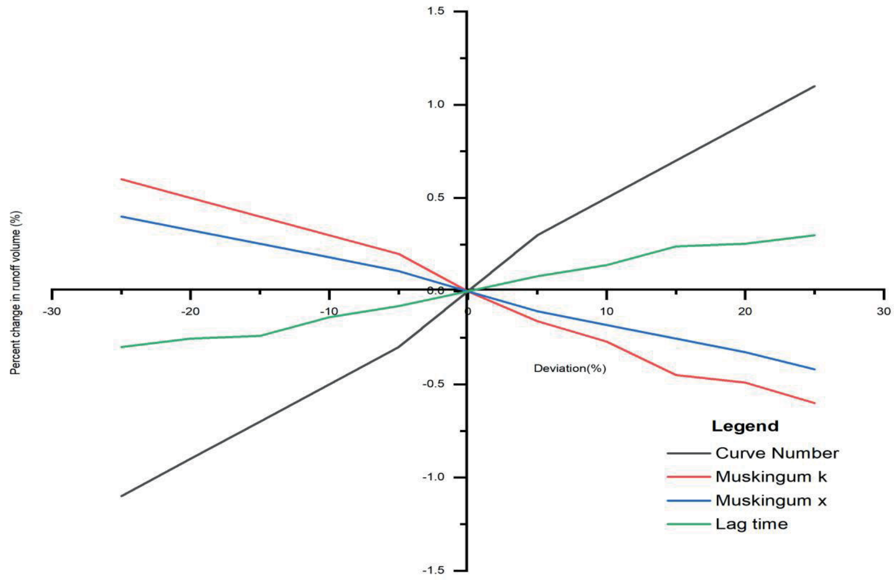

Fig. 8. Runoff change in response to parameter variation; source: own study

Table 4. Optimum value of Gilgel Gibe watershed physical parameters

Phases	Parameter value			
	t_{lag} (min)	Muskingum *k* (h)	Muskingum *x*	CN scale factor
Phase 1	238.514	3.641	0.234	0.905
Phase 2	235.530	3.484	0.216	0.876

Source: own study.

Table 5 shows the optimum values of the statistical test of error functions for both calibration phases.

Table 5. Optimum values of statistical tests of error functions during the model calibration period

Phase	Value of error functions				
	NSE	R^2	*RMSE* ($m^3 \cdot s^{-1}$)	*PBIAS* (%)	*PEP* (%)
1	0.780	0.949	27.990	3.500	−16.800
2	0.810	0.883	26.220	12.950	25.488
Mean	0.795	0.916	27.105	8.225	7.789

Source: own study.

The first phase of the model calibration result showed that the model well estimated the watershed runoff. The model slightly overestimated the simulated peak discharge during the first phase. The *PEP* value between the simulated and observed peak discharge was −16.8%. The negative sign indicates that the observed peak discharge was lower than the simulated peak discharge.

During the second phase, all the values of the statistical tests of error functions were improved except the *PBIAS* value, which went up 9.45% from the first phase. The model underestimated the observed peak discharge by 25.5% during the second phase. The higher values of *NSE* and R^2 and lower values of *PEP, PBIAS*, and *RMSE* indicate the better performance of the model during model calibration period.

Overall, the mean values of *NSE*, R^2, *RMSE, PBIAS* and *PEP* are 0.795, 0.916, 27.105 $m^3 \cdot s^{-1}$, 8.225%, and 7.789%, respectively. According to the category defined by Zou *et al.* [2003], the mean values of statistical test error functions for the two phases calibration period showed strong category of model performance. Moriasi *et al.* [2007] has also stated that if the value of *NSE* is greater than 0.75 during model calibration, the model performance is under a very good category. Therefore, the error function values obtained during model calibration period are under the acceptable level of accuracy.

The daily incremental precipitation, simulated and observed runoff hydrographs for both phases are shown in Figure 9a and b. Visual observation of the graphs indicates that the simulated runoff hydrograph is very close to the observed runoff hydrograph. The temporal variation of the two hydrographs is also similar. The graph from Figure 9a and b also shows more incremental rainfall causes more direct runoff. The correlation between the observed and simulated values of runoff for both phases of calibration periods are shown in Figure 10a and b. The figures indicate that the simulated and observed runoff values uniformly distributed around the trend line. This indicates the existence good correlation between the simulated and observed runoff values.

MODEL VALIDATION

During model validation, the simulated and observed runoff values were compared using the same criterion that was used for model calibration. Similar to the calibration period, the model validation period was divided into two different phases. The values of optimum parameters obtained from model calibration were directly used for model validation.

From 11 years of daily recent observed flow data to be used for model validation, six years (1 January 2003 to 31 December 2008) and the remaining five years (from 1 January 2009 to

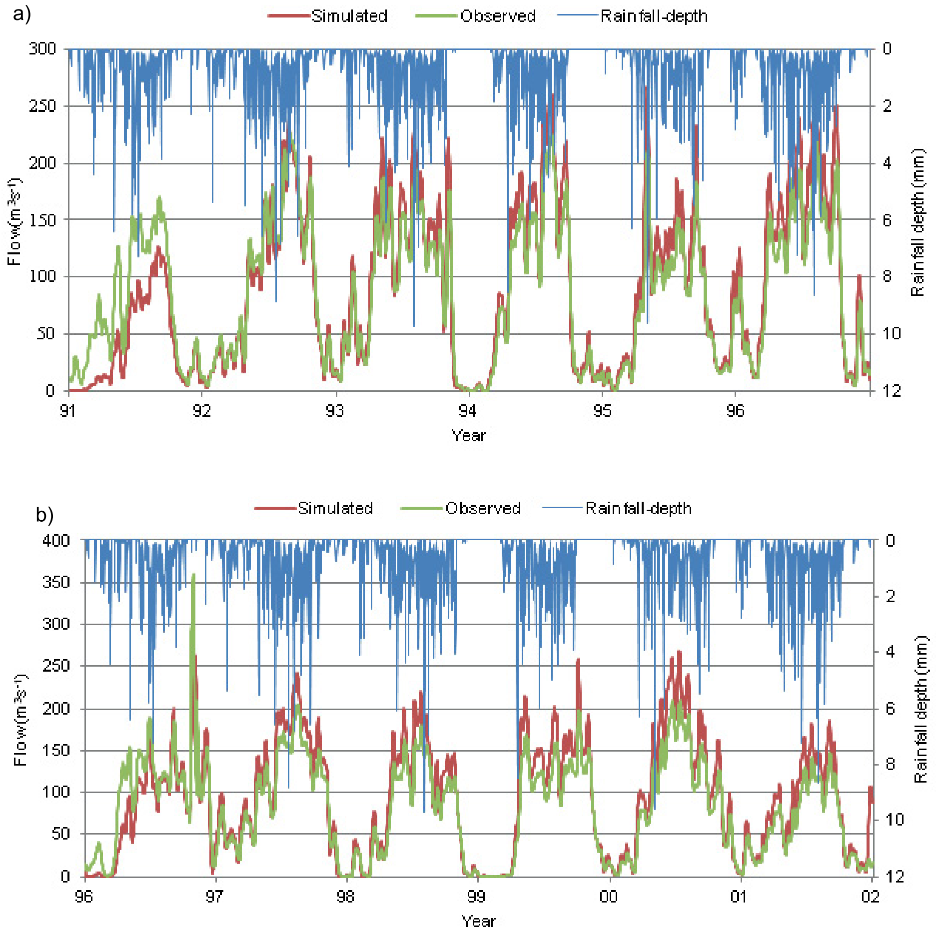

Fig. 9. Incremental precipitation graph, simulated and observed runoff hydrographs for calibration period: a) phase 1 and, b) phase 2; source: own study

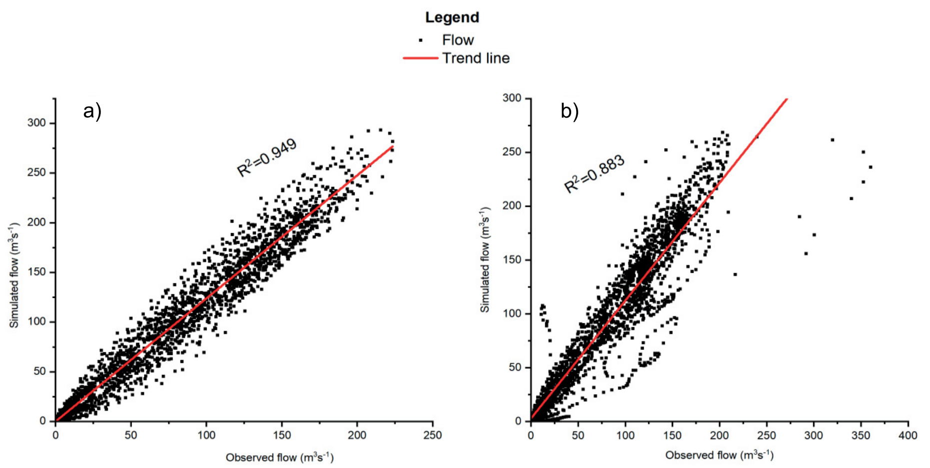

Fig. 10. Scattered plot of observed and simulated runoff values for calibration period: a) phase 1 and, b) phase 2; source: own study

31 December 2013) of observed flow data was used for the first and second phases of model validation periods, respectively.

The model validation result showed that the model performance value of *NSE* = 0.775 for the first phase was lower than the *NSE* value of the second phase (0.815). On the other hand, the first phase of R^2, *RMSE*, *PBIAS* and *PEP* values (0.948, 30.583 $m^3 \cdot s^{-1}$, 28.2%, and −28.175%, respectively) were higher than the second phase of R^2, *RMSE*, *PBIAS*, and *PEP* values (0.884, 17.830%, 28.512 $m^3 \cdot s^{-1}$ and −11.221%, respectively).

The result showed that the model performs well in the second phase of the validation period. The simulated value of peak discharge in the first phase was 237.90 $m^3 \cdot s^{-1}$, which is higher than the observed value of peak discharge (185.6 $m^3 \cdot s^{-1}$).

The second phase of the simulated value of peak discharge (447.45 $m^3 \cdot s^{-1}$) was also higher than the observed value of peak discharge (402.310 $m^3 \cdot s^{-1}$). However, the *PEP* value of the second phase (−11.221%) was lower than the first phase of *PEP* value (−28.175%). These results signified that the model overestimated the peak discharge in both phases, but it worked better in the second phase. Tassew *et al.* [2019] also got satisfactory values of statistical testes of error functions during model calibration using similar methods of transform, losses and channel routing.

Generally, the performance values of the error function in both phases were under the acceptable level of accuracy. The mean values of the error functions (*NSE* = 0.795, R^2 = 0.916, *RMSE* = 29.548 $m^3 \cdot s^{-1}$, *PBIAS* = 23.015% and *PEP* = –19.698%) for the two phases indicate that HEC-HMS model well estimated the daily runoff and peak discharge during the validation period. Other previous studies conducted on Upper Blue Nile River basin in Ethiopia by Sintayehu [2015] and Zelelew and Melese [2018] got satisfactory values of statistical tests of error function during the validation and calibration periods of event and continuous based simulation.

The performance values of the statistical tests of error functions during the validation period are summarized in Table 6. The daily simulated and observed runoff hydrographs and the graph of incremental precipitation for the two phases are shown in Figure 11a and b. The scattered plot of simulated and observed runoff values are shown in Figure 12. The similarity in trend and the closeness of the two hydrographs indicates the strength of the relationship between the simulated and observed runoff values.

The model calibration and validation result showed that HEC-HMS model has performed well in runoff simulation of Gilgel Gibe watershed. However, there was considerable difference between the simulated and observed runoff peak values in some years of the calibration and validation periods (Fig. 9 and 11). This may be due to: (1) The observed flow is taken near the outlet of the watershed and not exactly at the outlet of the watershed. (2) Four of the seven stations (Omo Nada, Dedo, Sekoru and Limu Genet) have more missing rainfall data in the year 1997, 2009, 2010 and 2011 which was filled using different data filling techniques. However, accurate data cannot be obtained by data filling techniques. (3) The curve number value is computed from LU/LC data of the year 2013 (The recent LU/LC is used for more precision). Therefore, the CN value associated with that event is not the actual CN value of that event. i.e temporal variation of CN value is assumed to be constant during this study. (4) The CN value for the LU/LC and soil type of the study area is assigned form the standardized Soil

Table 6. Optimum values of error functions during the model validation period

Phase	Value of error functions				
	NSE	R^2	*RMSE* (m^3s^{-1})	*PBIAS* (%)	*PEP* (%)
1	0.775	0.948	30.583	28.200	–28.175
2	0.815	0.884	28.512	17.830	–11.221
Mean	0.795	0.916	29.548	23.015	–19.698

Source: own study.

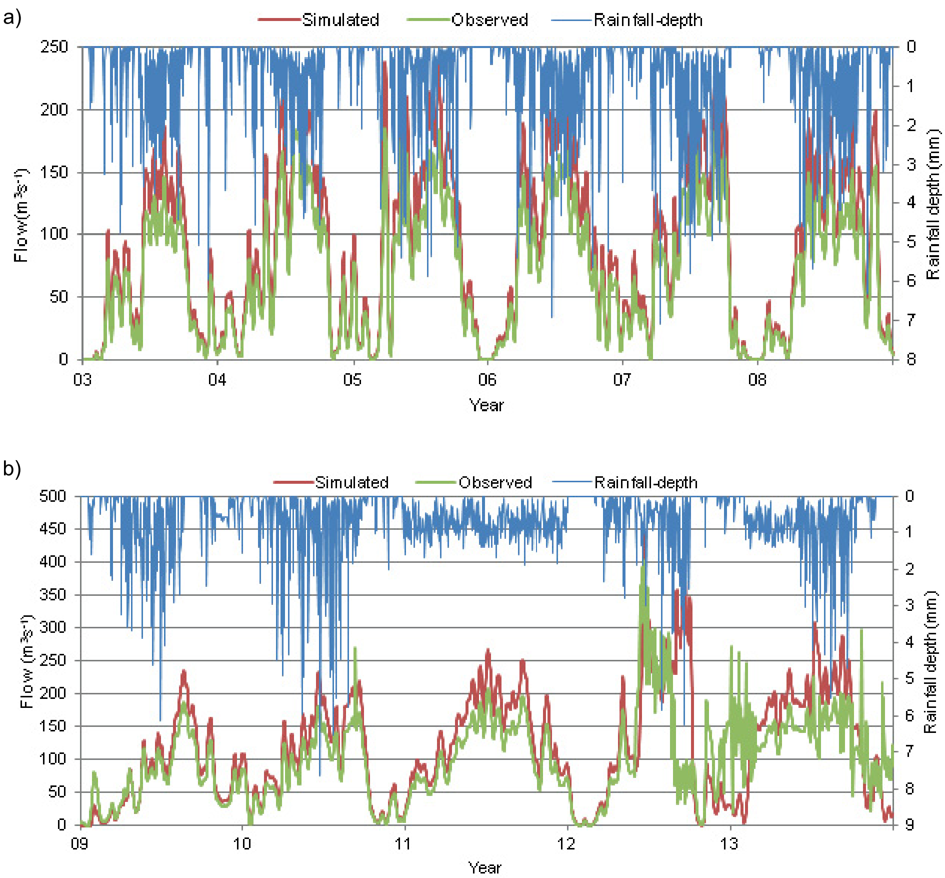

Fig. 11. Incremental precipitation graph, simulated and observed runoff hydrographs during the validation period: a) phase 1, and b) phase 2; source: own study

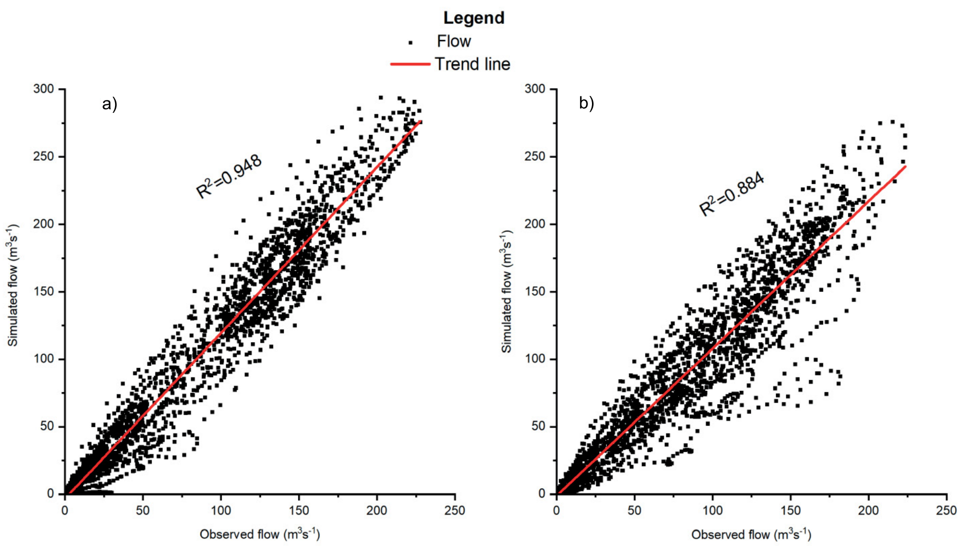

Fig. 12. Scattered plot of observed and simulated runoff for the validation period: a) phase 1, and b) phase 2; source: own study

Conservation Service Curve Number table which is developed from United States of small agricultural watershed [USACE 2010]. This does not represent the actual CN value of the Gilgel Gibe watershed. (5) HEC-HMS model has its own limitation associated with the methods of base flow, transform, channel routing and losses estimation [SKHAKHFA, OUERDACHI 2016; GUMINDOGA *et al.* 2017; HAMAD et al. 2021]. Due to these reasons, the model may not adequately simulate the response of rainfall in certain years. TASSEW et al. [2019]; SINTAYEHU [2015] proved the existence of minor underestimation of peak discharge by HEC-HMS model.

CONCLUSIONS

In this study, the performance of the HEC-HMS model was tested for continuous runoff simulation of Gilgel Gibe watershed. The sensitivity analysis indicated that curve number and wave travel time were the most sensitive parameters whereas, channel storage coefficient and lag time were moderately sensitive parameters.

The values of statistical testes of error functions during model evaluation showed the existence of good agreement between the simulated and observed runoff hydrograph. This indicates that the model well simulated the Gilgel Gibe watershed runoff. However, a minor difference existed between the simulated and observed values of the peak discharge during the calibration and validation period majorly due to absence of observed stream flow exactly at the outlet of the watershed, lack of considerable data quality and the limitations of the model itself.

From the analytical parts of the HEC-HMS model, the selected loss (SCS-CN), transform (SCS-UH), and routing (Muskingum *k*) models gave satisfactory runoff prediction of Gilgel Gibe watershed. Therefore, the study indicates that the HEC-HMS model fits for continuous runoff simulation of Gilgel Gibe watershed. It can also be used for other watersheds having similar physical characteristics with Gilgel Gibe watershed. However, the study does not consider the effect of temporal variation of LU/LC and other watershed parameters. Hence, further study should be conducted by selecting different combinations of losses, transform, and routing models with the temporal variation of LU/LC and other spatial parameters of the watershed.

REFERENCES

DERDOUR A., BOUANANI A., BABAHAMED K. 2018. Modelling rainfall--runoff relations using HEC-HMS in a semi-arid region: case study in Ain Sefra Watershed, Ksour Mountains (SW Algeria). Journal of Water and Land Development. Vol. 36 p. 45–55. DOI 10.2478/jwld-2018-0005.

DU J., QIAN L., RUI H., ZUO T., ZHENG D., XU Y., XU C.Y. 2012. Assessing the effects of urbanization on annual runoff and flood events using an integrated hydrological modeling system for Qinhuai River basin, China. Journal of Hydrology. Vol. 464–465 p. 127–139. DOI 10.1016/j.jhydrol.2012.06.057.

GUMINDOGA W., RWASOKA D.T., NHAPI I., DUBE T. 2017. Ungauged runoff simulation in Upper Manyame Catchment, Zimbabwe: Application of the HEC-HMS model. Physics and Chemistry of the Earth, Parts A/B/C. Vol. 100 p. 371–382. DOI 10.1016/j.pce.2016.05.002.

GYAWALI R., WATKIN S.D.W. 2013. Continuous hydrologic modeling of snow-affected watersheds in the Great Lakes basin using HEC-HMS. Journal of Hydrologic Engineering. Vol. 18. Iss. 1 p. 29–39. DOI 10.1061/(ASCE)HE.1943-5584.0000591.

HALWATURA D., NAJIM M.M.M. 2013. Application of the HEC-HMS model for runoff simulation in a tropical catchment. Environmental Modeling and Software. Vol. 46 p. 155–162. DOI 10.1016/j.envsoft.2013.03.006.

HAMDAN A.N.A., ALMUKTAR S., SCHOLZ M. 2021. Rainfall-runoff modeling using the HEC-HMS model for the Al-Adhaim River catchment, northern Iraq. Hydrology. Vol. 8. Iss. 2 p. 58. DOI 10.3390/hydrology8020058.

IBRAHIM-BATHIS K., AHMED S.A. 2016. Rainfall-runoff modelling of Doddahalla watershed – an application of HEC-HMS and SCN-CN in ungauged agricultural watershed. Arabian Journal of Geosciences. Vol. 9. Iss. 3. p. 170. DOI 10.1007/S12517-015--2228-2.

KHANIYA B., WANNIARACHCHI S., RATHNAYAKE U. 2017. Importance of hydrologic simulation for LIDs and BMPs design using HEC-

-HMS: A case demonstration. International Journal of Hydrology. Vol. 1. Iss. 5 p. 138–146. DOI 10.15406/ijh.2017.01.00027.

Kumarasamy K., Belmont P. 2018. Calibration parameter selection and watershed hydrology model evaluation in time and frequency domains. Water. Vol. 10. Iss. 6 p. 710. DOI 10.3390/w10060710.

Laouacheria F., Mansouri R. 2015. Comparison of WBNM and HEC-HMS for runoff hydrograph prediction in a small urban catchment. Water Resources Management. Vol. 29. Iss. 8 p. 2485–2501. DOI 10.1007/s11269-015-0953-7.

Majidi K. 2012.Simulation of rainfall-runoff process using Green-Ampt Method and HEC-HMS Model. International Journal of Hydraulic Engineering. Vol. 1. Iss. 1 p. 5–9. DOI 10.5923/j.ijhe.20120101.02.

McColl C., Aggett G. 2007. Land-use forecasting and hydrologic model integration for improved land-use decision support. Journal of Environmental Management. Vol. 84. Iss. 4 p. 494–512. DOI 10.1016/j.jenvman.2006.06.023.

Meresa H. 2019. Modelling of river flow in ungauged catchment using remote sensing data: application of the empirical (SCS-CN), Artificial Neural Network (ANN) and Hydrological Model (HEC-HMS). Modeling Earth System and Environment. Vol. 5 p. 257–273. DOI 10.1007/s40808-018-0532-z.

Mishra S.K., Singh V.P. 2013. Soil conservation service curve number (SCS-CN) methodology. Springer Science & Business Media. Vol. 42. Iss. 5 p. 84–146. DOI 10.1007/978-94-017-0147-1_2.

Moriasi D. N., Arnold J.G., Van Liew M W., Bingner R.L., Harmel R. D., Veith T.L. 2007. Model evaluation guidelines for systematic quantification of accuracy in watershed simulations. Transactions of the ASABE. Vol. 50. Iss. 3 p. 885–900. DOI 10.13031/2013.23153.

Pechlivanidis I.G., Jackson B.M., Mcintyre N.R., Wheater H.S. 2011. Catchment scale hydrological modelling: A review of model types, calibration approaches and uncertainty analysis methods in the context of recent developments in technology and applications. Global NEST Journal. Vol. 13. Iss. 3 p. 193–214. DOI 10.30955/gnj.000778.

Raes D., Willems P., Gbaguidi F. 2006. RAINBOW – A software package for hydrometeorological frequency analysis and testing the homogeneity of historical data sets. In: Proceedings of the 4th International Workshop on Sustainable Management of Marginal Drylands. Islamabad, Pakistan 27–31 January 2006. Vol. 2731 p. 12

Rahman K.U., Balkhair K.S., Almazroui M., Masood A. 2017. Sub-catchments flow losses computation using Muskingum--Cunge routing method and HEC-HMS GIS based techniques, case study of Wadi Al-Lith, Saudi Arabia. Modeling Earth System and Environment. Vol. 3. Iss. 4 p. 4. DOI 10.1007/s40808-017--0268-1.

Ramly S., Tahir W. 2015. Application of HEC-GeoHMS and HEC-HMS as rainfall–runoff model for flood simulation. In: Proceedings of International symposium on Flood Research and Management. Eds. W. Tahir, P. Abu Bakar, M. Wahid, S. Mohd Nasir, W. Lee. Springer, Singapore p. 181–192. DOI 10.1007/978-981-10-0500-8_15.

Roy D., Begam S., Ghosh S., Jana S. 2013. Calibration and validation of HEC-HMS model for a river basin in Eastern India [online]. ARPN Journal of Engineering and Applied Sciences. Vol. 8. Iss. 1 p. 40–56. [Access 27.03.2020]. Available at: http://www.arpnjournals.com/jeas/research_papers/rp_2013/jeas_0113_847.pdf

Scott H.D., Hofer K.R. 1995. Spatial and temporal analyses of the morphological and land use characteristics of the Buffalo River watershed [online]. University of Arkansas, Fayetteville Arkansas Water Resources Center P. 61 [Access 20. 05.2019]. Available at: https://core.ac.uk/download/pdf/127621942.pdf

Sintayehu L.G. 2015. Application of the HEC-HMS model for runoff simulation of upper Blue Nile River Basin. Hydrology: Current Research. Vol. 6. Iss. 2 p. 1–8. DOI 10.4172/2157-7587.1000199.

Skhakhfa I.D., Ouerdachi L. 2016. Hydrological modelling of wadi Ressoul watershed, Algeria, by HEC-HMS model. Journal of Water and Land Development. No. 31 p. 139–147. DOI 10.1515/jwld-2016-0045.

Song X.M., Kong F. Z., Zhu Z.X. 2011. Application of Muskingum routing method with variable parameters in ungauged basin. Water Science and Engineering. Vol. 4. Iss. 1 p. 1–12. DOI 10.3882/j.issn.1674-2370.2011.01.001.

Tassew B.G., Belete M.A., Miegel K. 2019. Application of HEC-HMS Model for flow simulation in the Lake Tana Basin: The case of Gilgel Abay Catchment, Upper Blue Nile Basin, Ethiopia. Hydrology. Vol. 6. Iss. 1 p. 21. DOI 10.3390/hydrology6010021.

Teklu N., Talema A., Mogessie E. 2016. Proceeding of The Second National Consultative Workshop on Integrated Watershed Management on Omo-Gibe Basin. Ethiopia [online]. [Access 17.05.2019]. Available at: https://www.researchgate.net/publication/313428353_Proceeding_of_The_Second_National_Consultative_Workshop_on_Integrated_Watershed_Management_of_Omo-Gibe_Basin

USACE 2010. Hydrologic modeling system (HEC-HMS). User's manual. Ver. 3.5 [online]. Davis, Calif. US Army Corps of Engineers, Hydrologic Engineering Center. [Access 23.02. 2019]. Available at: https://www.hec.usace.army.mil/software/hec-hms/documentation/HEC-HMS_Users_Manual_3.5.pdf

Verma A.K., Jha M.K., Mahana R.K. 2010. Evaluation of HEC-HMS and WEPP for simulating watershed runoff using remote sensing and geographical information system. Paddy Water and Environment. Vol. 8. Iss. 2 p. 131–144. DOI 10.1007/s10333-009--0192-8.

Wałęga A. 2013. Application of HEC-HMS programme for the reconstruction of a flood event in an un controlled basin [online]. Journal of Water and Land Development. Vol. 18 p. 13–20. [Access 04.05.2021] Available at: https://www.itp.edu.pl/JWLD/files/Walega_8hzpck8j.pdf.

Yener M.K., Sorman A.U., Sorman A.A., Sensoy A., Gezgin T. 2007. Modeling studies with HEC-HMS and runoff scenarios in Yuvacik Basin, Turkiye. International Congress on River Basin Management. Vol. 4 p. 621–634.

Zelelew D.G., Melesse A.M. 2018. Applicability of a spatially semi--distributed hydrological model for watershed scale runoff estimation in Northwest Ethiopia. Water. Vol. 10. Iss. 7. p. 923. DOI 10.3390/w10070923.

Zhang H.L., Wang Y.J., Wang Y.Q., Li D.X., Wang X.K. 2013. The effect of watershed scale on HEC-HMS calibrated parameters: A case study in the Clear Creek watershed in Iowa, US. Hydrology and Earth System Sciences. Vol. 17. Iss. 7 p. 2735–2745. DOI 10.5194/hess-17-2735-2013.

Zou K.H., Tuncali K., Silverman S.G. 2003. Correlation and simple linear regression. Radiology. Vol. 227. Iss. 3. p. 617–628. DOI 10.1148/radiol.2273011499.